Modeling L-Band Reflection and Emission From Seawater, Foam, and Whitecaps Using the Finite-Difference Time-Domain Method

Derek M. Burrage, Magdalena D. Anguelova, David W. Wang, and Joel C. Wesson

***Abstract*— Reflection and emission from flat and rough seas with embedded whitecaps (WCs) are investigated at L-band using a custom finite-difference time-domain electromagnetic model. The model is applied to multiple layers, with vertically inhomogeneous dielectric profiles representing foam and spray overlying a homogeneous seawater layer. The foam and spray layers are adapted from an L-band radiative transfer model, and the rough sea surface is a statistical realization of the Kudryavtsev wave spectrum model. The 1-D and 2-D model versions are validated for a flat sea with optional foam cover, and the emissivity effects of WCs embedded in flat and rough seas are investigated. An overlying spray layer is found to markedly reduce WC detectability. Possible applications are the stochastic simulation of WC cover and its effect on emissivity at various wind speeds, and the effects of wave and WC shape on emissivity.**

***Index Terms*— Emissivity, finite-difference time domain (FDTD), foam, radar cross section, reflectivity, seawater, spray, whitecaps (WCs).**

I. Introduction

FORMATION of whitecaps (WCs) due to waves breaking on a wind-roughened sea surface facilitates the exchange of mass, momentum, and heat between the atmosphere and ocean. It, thus, influences processes governing weather and climate such as the transfer of carbon dioxide, tropical convection and storm development, and ocean currents. Beginning at moderate wind speeds (exceeding about ∼4 m/s), breaking waves produce air bubble plumes at and below the surface, resulting in transient (active breaking) and persistent foam patches. In moderate to high winds, water droplets injected above the surface form spray layers that may obscure the surface [1]. Previous lab, field, and remote sensing studies empirically quantified parameters such as WC coverage and scale, foam layer thickness, and bubble profiles [2]. Only a few simulated roughness, foam and WC reflectivity r, and emissivity e use analytical and numerical electromagnetic (E-M) models (see [3], [4]). We report the development and application of a finite-difference time-domain (FDTD) E-M model to investigate emissivity, reflectivity, and detectability of WCs represented by patches of foam. The foam layer void fraction profile used in the 1-D radiative transfer model (RTM) of [5] is used to specify foam dielectric properties in the FDTD model. However, the E-M solution methods of these models, which run independently, are very different. The FDTD model generalizes the layer structure to a 2-D space that allows foam patches (WCs) of finite horizontal size to be studied.

The FDTD model solves Maxwell's equations directly for an arbitrary free space and dielectric configuration. It features an accurate E-M plane wave source with highly absorbing boundary conditions (ABCs), and an auxiliary near-to-far-field transformation (NTFT) for computing bistatic radar cross sections (BRCSs). Optional targets include an idealized perfect electric conductor (PEC), and single and multiple dielectric layers of foam and spray on a calm or rough sea water surface.

The simulation techniques follow previous FDTD studies applied to rough surface scattering, some with a floating or overlying object of interest (see [6] and references cited). Li *et al.* [6] extend by using a more realistic (non-Gaussian) wind-wave spectrum and a foam layer embedded in the sea surface. A focus on microwave L-band (wavelength, $\lambda \sim 21$ cm) allows scattering by microscale foam features, such as droplets and bubble clouds to be ignored. However, rigorous FDTD solution of Maxwell's equations allows modeling of single- and multiple-surface scattering, volume scattering, and WC edge diffraction effects, consistent with approximations limited only by grid resolution and available computer power (CPU and RAM).

II. Radiative Transfer Model

The RTM [5] computes sea surface emissivity using dielectric layers to represent a seawater half space and overlying foam layer for microwave frequencies of 1–37 GHz. It employs vertically inhomogeneous, and horizontally uniform and isotropic foam layers to derive complex dielectric constant profiles spanning foam layer depth. Foam layers are defined by a void fraction, Vf, profile varying exponentially between top and bottom limits. These few parameters, which determine only macroscopic foam characteristics, suffice to model emissivity; provided wavelengths are large enough compared to microscopic foam features that the volume scattering and diffraction within foam layers are negligible.

Based on the *Vf* profile, a seawater permittivity model and refractive (quadratic) mixing rule define the foam layer dielectric properties. The model produces emissivity estimates

Manuscript received June 8, 2018; revised September 11, 2018; accepted October 27, 2018. Date of publication November 30, 2018; date of current version April 22, 2019. This work was supported by the Office of Naval Research "Combined Use of Airborne Reflectometry and Radiometry to Retrieve Surface Winds, Waves and Wakes in Tropical Cyclones" research program under Program 0601153N. This is NRL contribution NRL/JA/7330-18-3998. *(Corresponding author: Derek M. Burrage.)*

D. M. Burrage, D. W. Wang, and J. C. Wesson are with the Naval Research Laboratory, Division of Oceanography, Stennis Space Center, MS 39529 USA (e-mail: derek.burrage@nrlssc.navy.mil; david.wang@nrlssc.navy.mil; joel.wesson@nrlssc.navy.mil).

M. D. Anguelova is with the Naval Research Laboratory, Division of Remote Sensing, Washington, DC 20375 USA (e-mail: maggie.anguelova@nrl.navy.mil).

Color versions of one or more of the figures in this letter are available online at http://ieeexplore.ieee.org.

Digital Object Identifier 10.1109/LGRS.2018.2881159

U.S. Government work not protected by U.S. copyright.

at 0°–90° incidence angles, and it accounts for up- and down-welling emissions within the seawater and foam, and multiple reflections at layer interfaces.

III. FDTD Model Implementation

The FDTD model is implemented in 1-D, 2-D, and 3-D versions using custom vectorized MATLAB code (The Mathworks Inc., Natick, MA, USA, 2016). It runs on an 8-core PC workstation with 24 GB of memory. Smaller runs can be accelerated using a graphics processing unit. This SURFace Emission and Reflection by Seawater And Foam model ("SURFER SAM" or SURFER for short) is based on algorithms described in [7], developed mainly to simulate interactions of E-M radiation with a rough sea surface; it is sufficiently general to probe targets of arbitrary geometry and dielectric structure using sinusoidal or pulsed point or plane wave sources. The main code, which includes interactive graphics, computes E-M fields, E and H. A separate "LYSFIELDS" MATLAB code that analyzes model runs implements an NTFT and produces BRCS plots from saved near-field boundary data. SURFER 1-D and 2-D versions were used in this letter, with embedded foam layers specifying the dielectric structure, as in RTM. (The SURFER 3-D code is in an advanced testing stage.)

A. Simulation Methods

The 1-D and 2-D FDTD algorithms [7] solve Maxwell's first-order coupled linear electric (E) and magnetic (H) field equations using the second-order explicit finite-difference procedure on a lattice supported by the Yee unit cell [8]. This cubic cell defines staggered E and H Cartesian field component locations and leap frog computation of E and H in time, and it satisfies Maxwell's divergence equations automatically. A right-handed orthogonal reference frame is used throughout this letter. In physical space, and in the plots, $+y$ is vertically upward, $+x$ is to the right, and $+z$ is out of the page. In SURFER 2-D, the incident wave propagates downward, but in SURFER 1-D, the physical space is rotated 90° anticlockwise so the propagation is to the right. Square cells were used in the 2-D model with size, dx, resolving E-M wavelength, $\lambda \sim 20$ cm at L-band, by a factor of at least 20, and the time step, dt, was chosen to guarantee Courant stability [7].

SURFER 2-D currently operates in transverse magnetic relative to $+z$ mode, with the Ez, Hx, and Hy Cartesian electric and magnetic field components (Ez, Hy in 1-D) defined positively with respect to their assigned axis directions, e.g., the horizontally polarized (H-pol) component, $+Ez$, points out of the page and lies parallel to the mean sea surface and perpendicular to the 2-D model domain. This contrasts with V-Pol, which requires dual transverse electric relative to $+z$ mode components (Hz, Ex, Ey); in 2-D, the two modes are uncoupled. The higher surface roughness sensitivity of H-pol is being used to study roughness influence on L-band sea surface salinity (SSS) retrievals.

To avoid internal reflections from the 2-D lattice boundaries, the convolutional perfectly matched layer (CPML) [7] is used as an ABC to absorb outgoing radiation at the boundary. After trials, we chose CPML layer thicknesses of 21 cells to attenuate strong outgoing radiation. This reduces internal field reflections by ~80 dB. For the 1-D model, Sullivan's simpler ABC approach [9] proved adequate.

To study surface reflections at various incidence angles, we apply the plane wave generator of the total field scattered field (TFSF) algorithm [7], along with a virtual TFSF free boundary (dashed line at cell $y = 305$, Fig. 3) lying in free space inside the CPML inner boundary. This separates the inside TF region (dark blue in Fig. 3) from the outside SF one (light blue). In both SURFER 1-D and 2-D, an auxiliary 1-D grid and lookup table are used to efficiently compute a source waveform along the TFSF boundary. To improve accuracy, the matched numerical dispersion method is used to correct directionally dependent grid dispersion [7]. This suppresses the incident wave Ez field in the SF region by ~60 dB. The incident plane wave source is a 1.413-GHz sine wave, chosen to approximate the narrow 27-MHz (2%) bandwidth, neutral H_2 line band protected for radio astronomy and radiometers sensing SSS, but broadband sources such as Fourier sums spanning several frequencies or a wideband pulse (e.g., Gaussian) can be used to span a discrete or continuous spectrum in a single model run.

B. Dielectric Formulation

Unlike PEC targets, seawater is a lossy dispersive medium with frequency-dependent complex dielectric constant and related properties. In SURFER, these properties can optionally be set at a particular frequency for narrowband studies using a selected seawater permittivity model, usually [10], which performs well in the L-band. For frequency-dependent broadband studies, SURFER optionally uses the auxiliary differential equation method [7] with a single-pole Debye formulation [10]. In either case, relevant dielectric properties are specified for known seawater salinity, S, and physical temperature, T. For all test runs (exceptions noted), $S = 35$ psu and $T = 25$ °C, and corresponding dielectric properties such as relaxation times, ionic conductivity, and Fresnel reflection coefficients were computed using [10], as needed.

C. Minimizing Edge Effects

Truncating the space lattice within the near field of the target necessitates the use of the CPML described earlier. We also use the plane wave generator along the TFSF interface. This works fine for a free-space TF region completely surrounding the target. However, complications arise for an extended target (the sea) filling an infinite half space. Where the target meets computational boundaries, it must stop immediately inside the TFSF or CPML boundary, or penetrate them to the outer edge of the space lattice. Spurious internal reflections can occur if care is not taken to minimize truncation artifacts.

Of the several approaches devised to alleviate spurious edge reflections, none appear simple to implement, sufficiently general, or fully effective. A simple but expensive approach of enlarging the TF region, so outgoing waves do not reach the boundary before the run stops, is often used to check the performance of other methods. The common incident wave tapering approach suppresses outgoing energy at model boundaries but needs incident power corrections. Fortunately, seawater is lossy, so we can confine artifacts to a small

near-surface area by restricting plane wave forcing at the TFSF boundary to the seawater penetration depth (∼1 cm at L-band). This reduces edge effects to an acceptable level.

D. Seawater, Foam, and Whitecap Representation

SURFER allows various domain configurations, but here, we use a space lattice with the CPML lining the outer boundary and a narrow free space SF region where field values can be probed. Inside its boundary, the TF region is filled with free space (air) in the upper half space and dielectric material (seawater, foam, and spray) in the lower half space (Figs. 1 and 3).

While SURFER 2-D was developed to study rough sea surface effects, we first report runs made with a flat surface. This allows comparisons of emissivity computed using SURFER, with RTM [5] and the algorithm [10], without the complications of rough surface emission, and provides a reference for determining the roughness emissivity increment. (In tests, flat PEC surfaces were used to validate SURFER using canonical targets with a known analytical response, e.g., a flat plate, or an infinitely long circular cylinder.)

In the 2-D model, WCs are represented by single or multiple patches of a horizontal foam layer of given thickness embedded within ambient seawater, so the upper surface remains smooth. In addition to foam layer parameters (thickness δm and void fraction, Vf, range), WC number, width, and spatial separation are specified. For initial tests, the sea surface was flat, allowing the essential WC response to be examined, without emissivity enhancement due to roughness. Then, the surface was roughened by varying its height horizontally to simulate random waves and demonstrate how roughness modifies the flat sea response. In this case, heights of the constant-thickness dielectric layers representing embedded foam and, optionally, overlying spray, were adjusted to conform to the rough surface profile. This imposed the rough surface shape on the WCs and revealed the quantitative impact of rough surface emission on WC detectability.

E. Spray Layer

An overlying spray layer reduces the depth of penetration into the seawater and any embedded foam patches (WCs). In this letter, we adapted the RTM foam layer formulation to add horizontally continuous spray layers to the FDTD model using δs and Vf ranges characteristic of spray. We then varied these parameters to study the impact on WC detectability.

IV. Model Validation

A. 1-D Model

The 1-D model is configured with Ez and Hy perpendicular to the propagation direction along the $x+$ axis (representing the vertical air/water column, but graphed horizontally). For the runs shown in Fig. 1, $dx = 1$ mm and the optional "magic" time step $dt = dx/(2c)$ [7], where c is the speed of light, were used. Seawater of depth 0.1 m (∼10 times penetration depth) with an optional embedded foam layer (WC) is overlaid by a spray layer beneath the free-space TFSF regions. As for the RTM, the foam void fraction, Vf, varied exponentially from 0.01 at its base to a specified value at its top (Table I). The

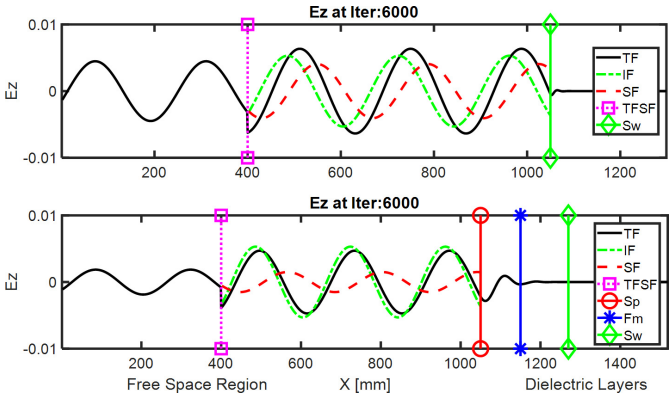

Fig. 1. Total, incident, and scattered Ez fields after 6000 iterations of 1-D model run for (Top) seawater only (Case 1) and (Bottom) seawater with overlying foam and spray (3). Vertical lines are tops of seawater, foam, and spray dielectric layers (solid line) and the NTFT virtual boundary (dotted line). See case details in Table I. Fm and Sp clearly limit penetration depth in case 3.

TABLE I
SURFER 1-D Emissivity Estimates for Spray and Foam-Covered Sea

#	δm	*Vf* Rng	δs	*Vf* Rng	*e*/*r*	Features
1	0	N. A.	0	N. A.	0.27/ 0.73	Seawater (S/w) only
2	12	0.60- 0.01	0	N. A.	0.50/ 0.50	Sw+Wet Foam
3	12	0.90- 0.01	10	0.90- 0.70	0.83/ 0.17	Sw+Thin Dry Spray +Thick Dry Foam
4	30	0.60- 0.01	50	0.97- 0.60	0.96/ 0.04	Thick Spray+Foam (Tropical Cyclone)

Emissivity and reflectivity (col 6) for given foam, δm, and spray thickness, δs [cm], (c 2, 4), and void fraction range (c 3, 5) for cases #1 - Seawater (Sw) only, #2 - Sw and wet foam #3 Sw plus thick dry foam and thin dry spray, #4 – Thick foam and spray (Tropical Cyclone) .

spray void fraction varied similarly but over a different range, optionally matched at the foam/spray boundary. There are few data to guide the spray range selection. We match it with the foam in case 4, but allow wetter spray overlying drier foam in case 3, despite its potential hydrostatic instability.

An L-band sine wave source of frequency 1.413 GHz ($\lambda =$ 21.1 cm) is specified at the TFSF virtual boundary (a point in SURFER 1-D). Then, consistency conditions remove the incident wave from the SF region. A probe in that region captures reflected Ez field values from which amplitude is derived. The squared ratio of reflected over incident wave amplitude determines the reflectivity r, and from Kirchhoff's energy conservation law, the emissivity $e = 1 - r$.

The SURFER 1-D model (Table I, Case 1) was validated by comparing the emissivity with the corresponding values computed from [10], and a close agreement was found. In that case, only seawater was present (no foam or spray layers). Model runs with and without a superimposed foam layer (1, 2) were also compared with the results for nadir incidence from the RTM model, and again, a close agreement was found.

B. 2-D Model

The extension to 2-D, while straightforward, introduces additional simulation features. Whereas SURFER 1-D is

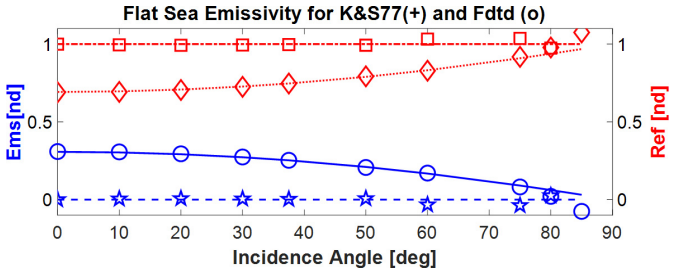

Fig. 2. Emissivity (blue circle) and reflectivity (red diamond) from SURFER 2-D for flat seawater compared with K&S77 [6] (solid and dotted lines). Modeled (star and square) and analytical values (dashed and dotted-dashed lines) for PEC flat plate.

confined to the nadir view, SURFER 2-D and the 1-D RTM admit nonzero incidence angles (0°–90°). Unlike RTM, SURFER 2-D allows dielectric layers of seawater, foam, and spray with rough surfaces to be defined. Otherwise, the 1-D and 2-D FDTD models share the same vertical layer structure. A more sophisticated spray layer RTM model is under test [11]. Pending its incorporation into SURFER, we adopt the current RTM foam layer here to represent spray; recognizing it provides only qualitative guidance on spray emissivity impact.

In the 2-D model, the temporal forcing is also sinusoidal, but a plane wave propagating at an incidence angle of 5° is applied around the TFSF boundary. Larger angles up to grazing incidence can be specified, but at the cost of longer run times. The auxiliary 1-D grid and lookup table are used to supply the source waveform [7]. The 2-D model is configured for propagation in the xy plane with $+z$ defining the H-Pol Ez component direction. The dielectric layer horizontal boundaries align with the x-axis and are assumed to be of infinite extent in the horizontal $+z$ direction (out of the page in Fig. 3). The space step $dx$is 2 mm and a magic time step dt is used.

The 2-D model validation was performed as for the 1-D model. However, runs were made over a range of incidence angles and for two different targets, a flat PEC plate and a seawater layer (without spray or foam). For the PEC target, SURFER 2-D closely matched the theoretical $r = 1$ value independent of incidence except near grazing incidence ($>75°$, Fig. 2) where some anomalies are seen and one value lies off scale, perhaps due to edge effects. For the seawater target, r varies from a minimum at nadir to a maximum near grazing (90°), and e varies in the opposite sense, consistent with Kirchhoff's law. There is a close agreement with flat sea emissivity values derived from [10], except near grazing incidence.

Comparisons were also made between RTM and SURFER, both using the RTM [5] foam layer structure, with Camps *et al.* [12] laboratory data (Table II). Foam thickness ($\delta m \sim 17$ mm) matched that in the lab, and the top of the Vf range of 0.01–0.385 was tuned to match the lab emissivity results. Deviations of the models (not shown) from the foam emissivity model of [12] were small, and only slightly larger for FDTD. Emissivity rms deviations across all incidence angles for F-R, F-C, and R-C (Table II) are 0.009, 0.029, and 0.020, respectively. Considering their different physical and numerical approximations, the RTM and FDTD models agree quite closely both with each other and with the data and model

TABLE II
COMPARING H-POL EMISSIVITIES FROM SURFER 2-D, RTM [1], AND LAB-GENERATED FOAM LAYER DATA [8]

Inc.Ang.	25	30	35	40	45	50
F	0.446	0.433	0.400	0.382	0.363	0.339
R	0.416	0.402	0.385	0.365	0.343	0.317
C	0.450	0.427	0.389	0.374	0.341	0.308
F-R	2.8	3.2	3.8	4.6	5.8	6.8
F-C	-5.1	-2.8	2.8	2.1	6.3	10.0
R-C	-7.6	-5.8	-0.9	-2.4	0.5	3.0

Emissivity (cols 2-7) for FDTD (F), RTM (R) and Camps Lab data (C) (rows 2-4) versus incidence angle. Deviation (%) of emissivities F from R (r. 5), F from C (r. 6) and R from C (r. 7). Models simulated lab conditions T=18.7 °C, S=33.21 and δm =17 mm. H-pol data for R and C adapted from [1 Fig 13]

of [12]. That model, however, requires more foam parameters than RTM [5].

V. RESULTS

SURFER 1-D was first run 22 times with seawater (necessarily flat in 1-D) and optionally overlying foam and spray layers of varying thicknesses and void fraction ranges. Four representative cases are shown in Table I. The validation cases of seawater (Case 1) and seawater with overlying thin wet foam (2) produced $r = 0.73$ and $e = 0.27$ and $r = 0.50$ and $e = 0.5$, respectively. Emissivity increases progressively as foam layer thickness or upper void fraction increases, and when a spray layer is superimposed (3), but as thickness exceeds E-M penetration depth, e asymptotes toward a limiting value. In the extreme case (4), representing a tropical cyclone, e approaches unity (0.96), as r is very low (0.04). Since the signal is mostly absorbed and, hence, re-emitted by spray, it barely reaches the foam or underlying seawater, which consequently play little or no role here in determining reflectivity or emissivity. In general, foam and spray provide an impedance match between seawater and free space and, thus, reduce surface reflectivity [13].

SURFER 2-D was then run, as described in the following, to study the emissivity and reflectivity of WCs and overlying spray, while taking care to minimize domain edge effects.

A. Effect of Whitecaps

A WC of width 80 cm [$\sim 4\lambda$, Fig. 3(a)] produces a distinctive emission pattern resembling radiation from a horizontal dipole or patch antenna, whereas an analog of the reflectivity response is a PEC plate with an x-centered z-parallel slot. The effect of a smaller 2.4-cm-diameter WC [Fig. 3(b)], though weaker, is still clearly discernable in the emission coefficient map. A multiplicity of randomly placed WCs [Fig. 3(d)] reveals a less distinctive overall response due to wave interference above the adjacent reflectors (or absorbers). In this short domain, some edge reflections appear from the $x^{+/-}$ directions, but the center probe location seems unaffected.

B. Effect of Overlying Spray

A spray layer overlying the 80-cm WC [Fig. 3(c)] increases overall emissivity near the surface from about 0.30 (above the Sw) or 0.50 (above the WC) to $e = 0.85$ [noting the expanded and shifted emissivity (Ems) color scale].

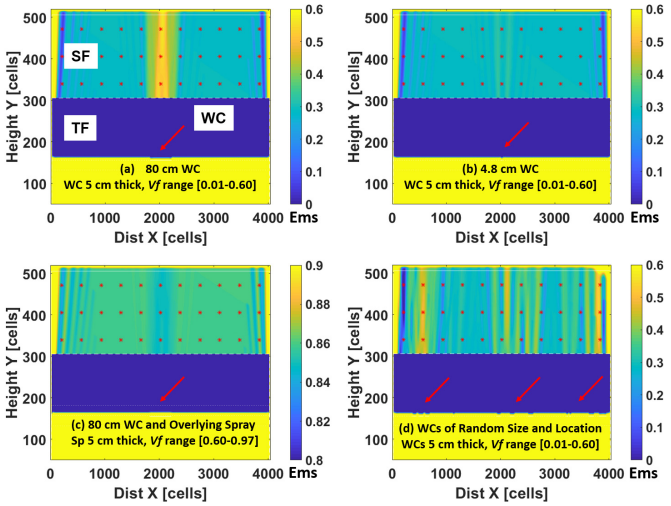

Fig. 3. SURFER 2-D simulation of emissivity (Ems) of (a) 80-cm WC, (b) 2.4-cm WC, (c) 80-cm WC with overlying spray (note expanded Ems color scale), and (d) randomly placed multiple WCs, over seawater. Locations of WCs (arrows) and probes (asterisks) highlighted in red. TFSF virtual surface at cell $Y = 305$. Layer parameters are also shown. $dx = 2$ mm.

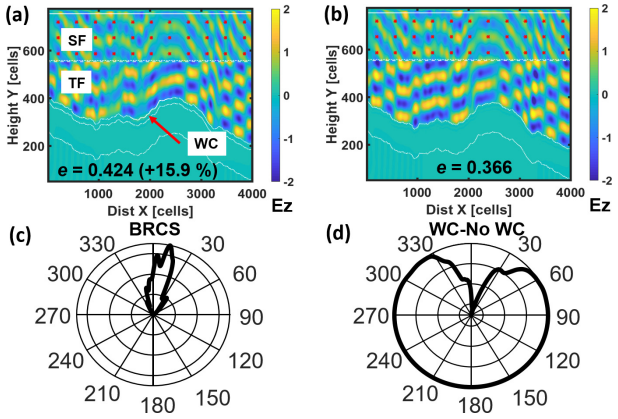

Fig. 4. SURFER Ez field for a rough sea surface with (a) 1.6-m-wide 5-cm-thick WC (20% cover) superimposed and (b) seawater only. (c) Nondimensional BRCS for (a) shows moderate reflectivity spanning $+/30°$ from zenith. (d) BRCS difference (a)–(b) with reduced r (higher e) due to WC.

It, thus, reduced the WC emissivity contrast and potentially its radiometric detectability (since the WC response is barely discernable).

C. Effect of Surface Roughness

In [4], [5], and [12] and in SURFER 1-D, a plane seawater–foam boundary is assumed. SURFER 2-D adds a capability to simultaneously model roughness and foam, and to show how diffuse reflections from a rough sea might obscure WC reflections. A single realization of a rough sea surface is shown with [Fig. 4(a)] and without [Fig. 4(b)] a WC present. This short surface profile was generated from the gravity wave spectrum [14] for a wind speed of 5 m/s with $T = 20$ °C and $S = 34$ psu. The WC reflections are barely evident in the Ez field plots. However, WC reflectivity and emissivity effects on a rough surface can be quantified using the NTFT [7], [15] to compute BRCS [Figs. 4(c) and (d)]. By differencing BRCS for the two runs, we clearly see an r reduction (e enhancement) in the forward scatter direction [Fig. 4(d)], with the WC present. Integrating the bistatic reflection coefficients about the unit circle shows emissivity increased from 0.366 to 0.424 (a 15.9% enhancement) when the WC was added. The effective emissivity depends on WC coverage (fractional width compared with model domain), which is itself a function of the WC scale and wind speed. Operational runs exploring this relationship over a range of wind speeds will be reported elsewhere.

VI. Conclusion

A new E-M model, SURFER, was developed to simulate microwave sea surface reflections and validated against semi-empirical and RT emissivity models. It was then used to study the emissivity effects of WCs, foam, and spray on a flat sea, and on a rough sea derived from a realistic gravity wave spectrum. Overlying spray layers dramatically increased the effective emissivity and markedly reduced WC detectability. A study of emissivity response to random wave and WC distributions versus wind speed is in progress, and simulations of nonlinear and breaking waves are also planned.

Acknowledgment

This is NRL contribution NRL/nn/7330-xx-xxx.

References

[1] L. H. Holthuijsen, M. D. Powell, and J. D. Pietrzak, "Wind and waves in extreme hurricanes, *J. Geophys. Res.*, vol. 117, no. C9, p. 15, 2012.
[2] E. A. Sharkov, *Breaking Ocean Waves*. Berlin, Germany: Springer, 2007, p. 278.
[3] J. T. Johnson and M. Zhang, "Theoretical study of the small slope approximation for ocean polarimetric thermal emission," *IEEE Trans. Geosci. Remote Sens.*, vol. 37, no. 5, pp. 2305–2316, Sep. 1999.
[4] V. Raizer, "Macroscopic foam–spray models for ocean microwave radiometry," *IEEE Trans. Geosci. Remote Sens.*, vol. 45, no. 10, pp. 3138–3144, Oct. 2007.
[5] M. D. Anguelova and P. W. Gaiser, "Microwave emissivity of sea foam layers with vertically inhomogeneous dielectric properties," *Remote Sens. Environ.*, vol. 139, pp. 81–96, Dec. 2013.
[6] L. Juan, G. Li-Xin, J. Yong-Chang, and J. Chun-Gang, "Frequency response of 1D dispersive sea surface by the ADE-FDTD algorithm," *Waves Random Complex Media*, vol. 22, no. 2, pp. 305–316, 2012.
[7] A. Taflove and S. C. Hagness, *Computational Electrodynamics: The Finite-Difference Time-Domain Method*, 3rd ed. Norwood, MA, USA: Artech House, 2005, p. 1006.
[8] K. S. Yee, "Numerical solution of initial boundary value problems involving Maxwell's equations in isotropic media," *IEEE Trans. Antennas Propag.*, vol. AP-14, no. 3, pp. 302–307, May 1966.
[9] D. M. Sullivan, *Electromagnetic Simulation Using the FDTD Method*. Hoboken, NJ, USA: Wiley, 2000, p. 165.
[10] L. A. Klein and C. T. Swift, "An improved model for the dielectric constant of sea water at microwave frequencies," *IEEE J. Ocean. Eng.*, vol. OE-2, no. 1, pp. 104–111, Jan. 1977.
[11] M. A. Anguelova and M. H. Bettenhausen, *Effect of a Sea Spray Layer on L-Band Signal From Ocean Surface*. Ann Arbor, MI, USA: GNSS+R, 2017. [Online]. Available: http://www.gnssr2017.org/images/Postersession/
[12] A. Camps *et al.*, "The emissivity of foam-covered water surface at L-band: Theoretical modeling and experimental results from the FROG 2003 field experiment," *IEEE Trans. Geosci. Remote Sens.*, vol. 43, no. 5, pp. 925–937, May 2005.
[13] M. D. Anguelova and P. W. Gaiser, "Dielectric and radiative properties of sea foam at microwave frequencies: Conceptual understanding of foam emissivity," *Remote Sens.*, vol. 4, no. 5, pp. 1162–1189, 2012.
[14] V. N. Kudryavtsev, V. K. Makin, and B. Chapron, "Coupled sea surface-atmosphere model: 2. Spectrum of short wind waves," *J. Geophys. Res.*, vol. 104, no. C4, pp. 7625–7639, 1999.
[15] J. B. Schneider. *Understanding the Finite-Difference Time-Domain Method*. Accessed: Sep. 10, 2018. [Online]. Available: http://www.eecs.wsu.edu/ schneidj/ ufdtd/ufdtd.pdf